

Shower X_{max} determination based on LOFAR radio measurements

STIJN BUITINK^{1,2}, ARTHUR CORSTANJE², J. EMILIO ENRIQUEZ², HEINO FALCKE^{2,3}, WILFRED FRIESWIJK³, JÖRG R. HÖRANDEL², MARIA KRAUSE², ANNA NELLES^{2,4}, PIM SCHELLART², OLAF SCHOLTEN¹, SATYENDRA THOUDAM², SANDER TER VEEN² AND MARTIN VAN DEN AKKER² FOR THE LOFAR COLLABORATION.

¹ *KVI, University of Groningen, 9747 AA Groningen, The Netherlands*

² *Department of Astrophysics/IMAPP, Radboud University Nijmegen, 6500 GL Nijmegen, The Netherlands*

³ *Netherlands Institute for Radio Astronomy (ASTRON), 7990 AA Dwingeloo, The Netherlands*

⁴ *Nikhef, Science Park Amsterdam, 1098 XG Amsterdam, The Netherlands*

s.j.buitink@rug.nl

Abstract: LOFAR is a multipurpose radio telescope which can be used for radio detection of cosmic rays while running astronomical observations at the same time. The core of LOFAR contains 2300 antennas within an area of four square kilometer. This high density makes it an ideal location for a detailed study of the radio signal of extensive air showers in the energy range 10^{16} - 10^{18} eV. The LORA scintillator array is located at the center of LOFAR and provides a trigger for the system and a reconstruction of the shower parameters.

We present an analysis of high quality LOFAR events for which the lateral distribution of the radio signal can be studied in 2D. For each event dedicated simulation sets for proton and iron primaries have been produced. The radio and particle data are fitted simultaneously to the simulation. This leads to a reconstruction of the depth of the shower maximum X_{max}, which opens the possibility for cosmic ray composition studies at energies exceeding 10^{16} eV.

Keywords: air showers, radio emission, experiments, LOFAR

1 Introduction

The last decade has seen a rapid development of the technique of radio detection of cosmic rays (CRs). The LOFAR prototype station LOPES demonstrated that air shower radio pulses are produced by a coherent mechanism driven by the Earth's magnetic field [1]. The power of the pulse is proportional to the square of the primary energy, providing excellent energy reconstruction for CRs above 10^{16} eV. Furthermore, the smoothness of the radio front allows a better angular resolution than can typically be achieved with particle detectors. Most importantly however, simulations have shown that the signal contains information about the atmospheric depth of the shower maximum (X_{\max}). This makes the technique a powerful alternative to fluorescence measurements which can only be conducted during dark moonless nights and have a duty cycle of less than 15% [2]. The air shower radio mechanism is known to be influenced by the electric fields in thunderstorms [3], but is reliable under other atmospheric circumstances.

While various experiments, including CODALEMA [4] and AERA [5], have made progress in measuring and understanding the properties of air shower emission, so far no X_{\max} measurements have been achieved with an accuracy comparable to the fluorescence technique. Here, we show that LOFAR is now capable of determining X_{\max} based on the very detailed measurements of the air shower radiation profile on the ground.

The Low Frequency Array (LOFAR) [6] is a digital radio telescope consisting of thousands of omni-directional dipole antennas spread out over the North of the Netherlands and some international stations in neighboring countries. It is the first telescope that has been designed to measure transient radio sources, including CRs. Each antenna is equipped with a buffer board, which can store one 1.3 s of data at 200 MHz sampling rate. This allows pointing of the

telescope towards any direction in the sky after the event has happened.

The antenna placement is very different from the regular grids common to astroparticle experiments. Since interferometry benefits from many different baselines, the antennas are grouped in stations which are logarithmically spaced. In the densely populated core, these stations are very close together. Air showers are often simultaneously observed by 5 to 9 stations, i.e. 250-500 antennas. The core is augmented with a small scintillator array LORA [7] that provides an air shower trigger and energy reconstruction. Together, LOFAR and LORA form a high-precision, hybrid CR observatory [8]. In the analysis presented here, we combine the radio and particle data to first optimize the shower core position, and then reconstruct X_{\max} . We present an example shower that has been measured at the 31st of July 2012 by 6 core LOFAR stations.

2 Method

The LORA particle array is configured to send triggers at a rate of 0.8 hr^{-1} and an energy threshold of $\sim 2 \times 10^{16}$ eV. When the system is triggered, the buffers of all antennas in the core are read out and stored. A data pipeline has been implemented that removes man-made radio interference sources from the data and performs several cycles of calibration and pulse recovery [9, 10]. Stations are selected for further data analysis when enough antennas find a radio pulse in the correct time window.

In this analysis we study the total power of the radio signal on the ground. This parameter is more robust than the maximum pulse amplitude, since it does not depend on the phase response of the antenna components. The distribution of the radio power on the ground is a complex function because of the interference of geomagnetic and charge ex-

cess radiation. To fully capture all the information that is encoded in this pattern it is not sufficient to fit a lateral distribution function (LDF): all azimuthal asymmetry would be averaged out. Instead, we fit a two-dimensional distribution function (2DF), which is acquired by interpolating simulation results. In these 2DFs the center corresponds to the shower core position, which, in general, does not coincide with the location where the radio pulse power reaches its maximum value.

Several codes are now available for the production of air shower radio simulation. Programs like CoREAS [11], ZHAireS [12], and EVA [13] simulate a combination of effects, like geomagnetic radiation, charge excess radiation, and the Cherenkov-like propagational effects that arise when including a realistic index of refraction of the atmosphere. Microscopic codes that treat each particle individually (CoREAS, ZHAireS) and macroscopic codes that calculate the global charge and current distributions (EVA) are converging towards similar results [14]. Here, we use CoREAS, which is a radio extension to CORSIKA [15]. This allows us to generate radio and particle output for each individual shower simulation.

For each high-quality LOFAR event we generate simulations of 25 protons and 15 iron showers. We use the QGSJETII and Fluka interaction models. The radio pulse is calculated for 160 positions on the ground. The power between these points is found by interpolation. For this interpolation to work properly, the locations must be chosen strategically. Since the radiation pattern is not rotationally symmetric around the shower axis, it is important to know at what angles the radiation reaches its maximum and minimum. The asymmetry arises from the vector sum of the two radiation components. While both mechanisms produce linearly polarized emission, their polarization angle is different. The geomagnetic component is always polarized in the $\mathbf{v} \times \mathbf{B}$ plane, where \mathbf{v} is the direction of propagation of the shower and \mathbf{B} is the magnetic field. The charge excess component, on the other hand, has a polarization radially outwards with respect to the shower axis. The interference is therefore completely constructive or destructive along the direction of $\mathbf{v} \times \mathbf{B}$ vector and reaches intermediate values at other angles. The pattern of ground positions that we use for simulations is a star-shaped pattern with two of its arms lying along the projected $\mathbf{v} \times \mathbf{B}$ axis. Note that the physical location of the positions in ground coordinates is therefore different for each event, depending on the arrival direction of the air shower.

The interpolated 2DF is plotted in Fig. 1. The small circles indicate the positions for which the radiation was simulated. Note that the maximum radio power is reached to the right of the shower core, while a deficit is visible to the left along the $\mathbf{v} \times \mathbf{B}$ axis.

The antenna gain of LOFAR antennas is given by a complex 2x2 Jones matrix that describes how the two on-sky polarizations are received as two instrumental polarizations [9]. To compare data to simulations we can either apply the inverted Jones matrix to the data, which gives the ‘physical’ signal, or apply the Jones matrix to the simulation to acquire the simulated received signal. While the two seem equivalent there is a subtle difference with respect to the way the background noise is treated. The antenna response depends on the arrival direction of the signal. When applying the inverted Jones matrix corresponding to the reconstructed arrival direction of the air shower to the data, one implicitly assumes that the background noise also

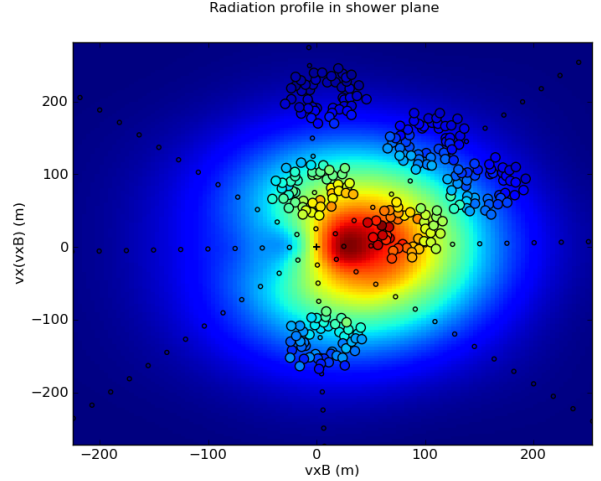


Figure 1: Projection of the two-dimensional radio power distribution on the shower plane. The x axis is in the direction of the $\mathbf{v} \times \mathbf{B}$ vector. The background colors represent the interpolated simulation results for a proton shower with $X_{\max} = 650 \text{ g/cm}^2$. The large circles represent the LOFAR antennas and their colors the received power. The small circles indicate the locations for which the radio signal was simulated. The shower core is located at the origin, indicated with a +. Its location is found by fitting the radio and particle data simultaneously. The power scaling is arbitrary.

comes from this direction. Since the background consists of contributions from all directions this assumption is false, and the noise is not transformed correctly. Especially for polarized emission this can lead to wrong values for the signal-to-noise ratio. This issue does not exist when applying the Jones matrix to the simulated data, since the simulation has no noise included. We therefore choose to apply the antenna model to the simulation and compare total received power. This includes a bandpass filter in the range 30–80 MHz.

We now fit the simulation to the radio and particle data simultaneously by minimizing:

$$\chi^2 = \sum_{\text{antennas}} \left(\frac{P_{\text{lofar}} - f_r P_{\text{sim}}(x_{\text{ant}} + x_{\text{off}}, y_{\text{ant}} + y_{\text{off}})}{\sigma_{\text{lofar}}} \right)^2 + \sum_{\text{stations}} \left(\frac{d_{\text{lora}} - f_p d_{\text{sim}}(x_{\text{stat}} + x_{\text{off}}, y_{\text{stat}} + y_{\text{off}})}{\sigma_{\text{lora}}} \right)^2, \quad (1)$$

where P_{lofar} is the power measured at an antenna at location $(x_{\text{ant}}, y_{\text{ant}})$ with noise level σ_{lofar} , P_{sim} is the simulated power, d_{lora} is the particle density as measured by a LORA detector at location $(x_{\text{stat}}, y_{\text{stat}})$ with noise σ_{lora} , and d_{sim} is the CORSIKA particle density. The fit has four free parameters: the core offset $(x_{\text{off}}, y_{\text{off}})$, and scaling factors f_r and f_p for the radio and particle distribution functions. The radio scaling is needed because the LOFAR data has no absolute calibration yet, while the particle density scaling is used because the energy of the simulated event is in general different from the real energy. The fitted core position is then used to obtain an updated energy estimate from LORA.

For each of the 40 shower simulations, this procedure is repeated. Since the direction and energy of the primary particle is kept constant, these showers represent the natural

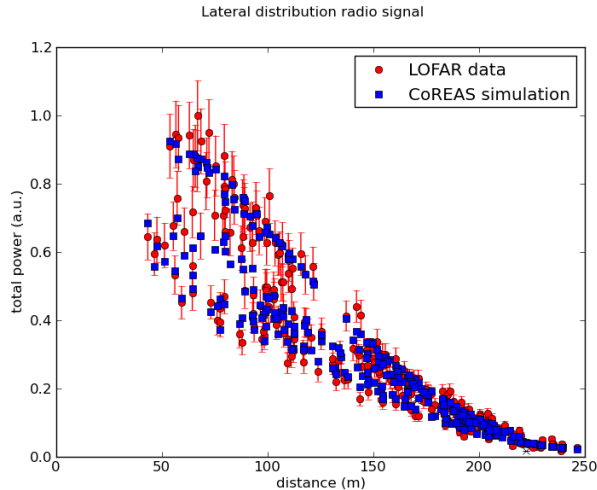


Figure 2: Radio power (data in red circles, simulation in blue boxes) plotted against core distance. Because of asymmetry in the radiation profile, the received power does not depend on distance to the shower core alone. Note the ellipsoid structure between 50 and 100 m; this corresponds to the station directly above the center in Fig. 1.

shower-to-shower fluctuations that arise from variations in the first interactions. The best fitting simulation is a proton shower with $X_{\max} = 650 \text{ g/cm}^2$. The corresponding 2DF is plotted in Fig. 1, while in Fig. 2 the measured and simulated power is plotted as a function of distance to the shower core. The complex structure of the data is very accurately reproduced by the simulation. The circular structure of the LOFAR stations can be recognized in the ellipsoidal shape in Fig. 2 between 50 m and 100 m core distance.

The effects of the core shift on the LORA LDF is shown in Fig. 3. The red circles indicate the core distances corresponding to the shower core position that was found by the original LORA reconstruction. The red solid curve is an NKG fit to this data. The updated core distances are given by the blue squares. The blue dashed line corresponds to the actual charged particle density that was generated in the CORSIKA simulation, scaled by a factor f_p . Most of the LORA stations have an increased core distance in the new fit, leading to an increased energy estimate.

The location of the optimized core position depends on the particular simulated shower, as shown in Fig. 4. The data points indicate the offset with respect to the original core position. Their colors reflect the value of X_{\max} ; the very deep proton shower in red are in the top right corner, while the shallowest iron showers in blue are in the bottom right. Larger data points have a better overall fit quality. The best fitting shower is indicated with a star.

The core offsets are of the order of 50 m. This value seems large in view of the core reconstruction precision of LORA [7]. The reason for this apparent discrepancy is that the core falls outside of the particle array. In a LORA-only analysis such an event would not survive the quality cuts. In this combined analysis, however, the event is perfectly useful, and the LORA data complements the radio data.

The best fitting simulation yields $\chi^2/\text{ndf}=1.27$, which indicates that the model describes the data incredibly well. In general, many high quality LOFAR events fit to the simulation with $\chi^2/\text{ndf} < 2$. When thunderstorm conditions

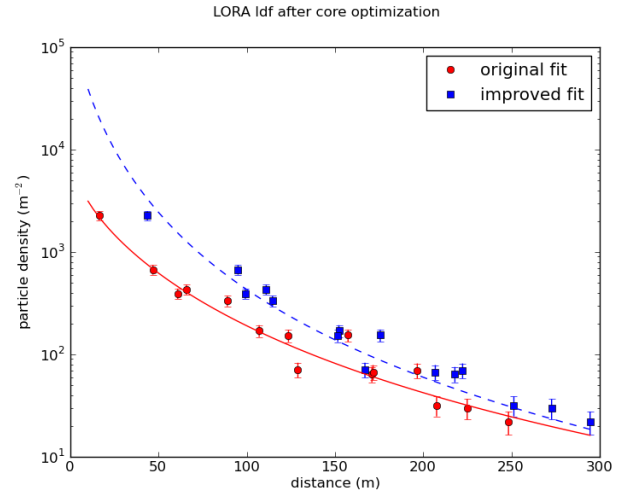


Figure 3: The original LORA LDF fit is given by red circles and corresponding curve. The blue squares correspond to the updated core distances of the LORA stations after the combined fit. The blue dashed line is the charged particle distribution of the CORSIKA output of the best fitting simulated shower, scaled by a factor f_p .

are present, however, the quality of the fit dramatically decreases. This is most likely due to the influence of atmospheric electric fields on the radiation [16].

3 Conclusions

We presented a new method to reconstruct the X_{\max} of air showers detected by LOFAR and LORA based on sets of radio simulations. For the example shower in this paper, we found a best fit to a proton shower with $X_{\max} = 650 \text{ g/cm}^2$. The sensitivity to the shower depth allows LOFAR studies of the CR mass composition in the energy range between 10^{16} eV and 10^{18} eV. This is an area of much interest that covers the iron knee [17] and reaches up to the ankle of the cosmic rays spectrum. The method is independent from that of other experiments that cover this range, such as KASCADE-Grande [18] and HEAT [19], and will complement their results.

Presently, only the total power of the signal has been used in the analysis. The method can be extended to include polarization and timing of the radio pulse [20] to improve its accuracy.

Acknowledgment: We acknowledge financial support from the Netherlands Organization for Scientific Research (NWO), VENI grant 639-041-130, the Netherlands Research School for Astronomy (NOVA), the Samenwerkingsverband Noord-Nederland (SNN) and the Foundation for Fundamental Research on Matter (FOM). LOFAR, the Low Frequency Array designed and constructed by ASTRON, has facilities in several countries, that are owned by various parties (each with their own funding sources), and that are collectively operated by the International LOFAR Telescope (ILT) foundation under a joint scientific policy.

References

- [1] H. Falcke et al., Nature 435, 313 (2005).
- [2] J. Abraham et al., [Pierre-Auger-Collaboration], NIMPA 523, 50 (2004).

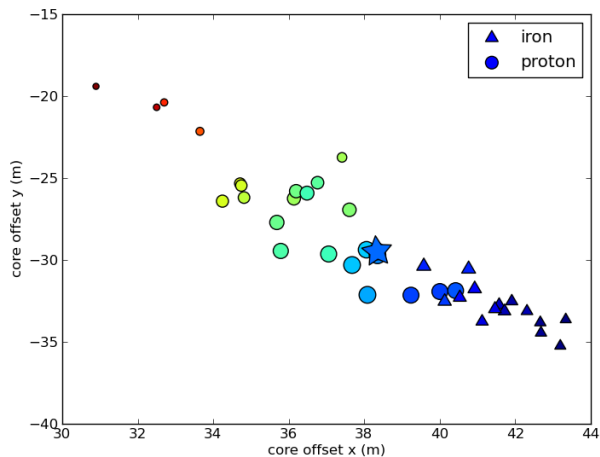


Figure 4: The values for (x_{off}, y_{off}) found in the optimization procedure for all forty shower simulations. The color of the data points represents the X_{\max} of that particular shower (blue = low, red = high). The size of the data points represent the quality of the fit. The best fitting proton shower is indicated with a star.

- [3] S. Buitink et al., A&A 467, 385 (2007).
- [4] D. Ardouin, et al., Astropart. Phys. 26, 341 (2006).
- [5] B. Fuchs et al. [Pierre-Auger-Collaboration], NIMPA 692, 93 (2012).
- [6] M. van Haarlem et al, LOFAR: The LOw-Frequency ARray, Accepted for Publication in A&A.
- [7] S. Thoudam et al., ASTRA 7, 195 (2011).
- [8] J. R. Hörandel for the LOFAR Collaboration, These Proceedings.
- [9] P. Schellart et al, [LOFAR collaboration] Detecting Cosmic Rays with a Radio Telescope, Submitted to A&A.
- [10] A. Nelles for the LOFAR Collaboration, These Proceedings.
- [11] T. Huege, M. Ludwig, and C. James, Proc. of the ARENA, Erlangen, Germany (2012).
- [12] J. Álvarez-Muñiz et al., Astropart. Phys. 35, 325 (2012).
- [13] O. Scholten et al., Astropart. Phys. 29, 94 (2008).
- [14] T. Huege et al., NIMPA 662, 179 (2012).
- [15] D. Heck et al., Report FZKA 6019 (1998).
- [16] S. Buitink et al., Astropart. Phys. 33, 296 (2010).
- [17] W. Apel et al. [KASCADE-Grande collaboration], PRL 107, 1104 (2011).
- [18] W. Apel et al. [KASCADE-Grande collaboration], PRD 87, 1101 (2013).
- [19] C. Meurer et al. [Pierre-Auger-Collaboration], ASTRA 7 183 (2011).
- [20] P. Schellart for the LOFAR Collaboration, These Proceedings.